J Fail. Anal. and Preven.
https://doi.org/10.1007/s11668-022-01489-4

TECHNICAL ARTICLE—PEER-REVIEWED

Investigation on Offshore Floating Mooring Chains Failure

S. Salem · I. El-Mahallawi · M. Shazly · H. Abouzeid · A. Elbshbeshy · Y. Reda

Submitted: 6 October 2022 / Accepted: 12 October 2022

Abstract The mooring system is essential for floating structures withstanding harsh environmental conditions, such as corrosion and variant wave loads. Failures of mooring systems has attracted researchers in different fields related to on-shore and off-shore activities. In this work, a study is conducted on a failed chain by conventional metallurgical failure analysis procedure including chemical analysis, tensile testing, and fracture surface examination. The studied samples included the failed section and samples from further region away from the failure. A 3D simulation model for the chain was demonstrated using ABAQUS Simula 2018. The results show that the maximum Von-Mises stress is around 790 MPa which exceeds the breaking load of R3 steel. On the other hand, using R4 steel, which has a higher UTS of 860 MPa, would have assured a safer design as the stresses generated at the same conditions are lower than the breaking load of R4 steel, compared to R3 steel. The microstructure confirmed that the material is low carbon alloy steel with ferrite and perlite grains along with iron oxide pits, which would be presumed to have made the material rather brittle. Despite the fracture of the tensile samples showed ductile features, the fractographic analysis of the failed part reveals that the chain was fractured catastrophically in a brittle manner. FEA results are in accordance with the fractographic analysis. Finite element analysis of R3 steel shows that the stress magnitude caused by out of plane bending (OPB) forces is 15% greater than that of ultimate tensile strength.

Keywords Mooring chains · Failure analysis case study · Finite element analysis

S. Salem (✉) · I. El-Mahallawi · M. Shazly · H. Abouzeid · A. Elbshbeshy
Mechanical Engineering Department, The British University in Egypt, Cairo, Egypt
e-mail: serag.salem@bue.edu.eg

I. El-Mahallawi
Metallurgical Engineering, Cairo University, Giza, Egypt

Y. Reda
Canal High Institute of Engineering and Technology, Suez, Egypt

Introduction

Under the seabed, the ocean offers us important natural resources, such as oil and gas. There are two types of structurers: fixed and floating structures. The exploration of oil and gas has moved to offshore areas and in deeper water, floating structure was found to be more appealing as it is cheaper compared to fixed structures. Therefore, the development of offshore floating structures is critical for the processing and storage of oil and gas industry [1]. Mooring system is an essential and critical part of the floating structure as it limits the movement of the floating structures ensuring its continuous operability. Moreover, the mooring system is required to withstand harsh environmental conditions, such as corrosion and variant wave loads.

Mooring systems consist mainly of an anchor, buoy, mooring lines, and connectors. They have different categories depending on the configuration of the system which could be grouped into taut leg mooring systems or catenary mooring systems, see Fig. 1. The factors that determine the type of mooring include the depth of deployed waters, cost factors, and deployment strategy [2]. The mooring line (chain and/or cable) is one of the most important

Published online: 27 October 2022

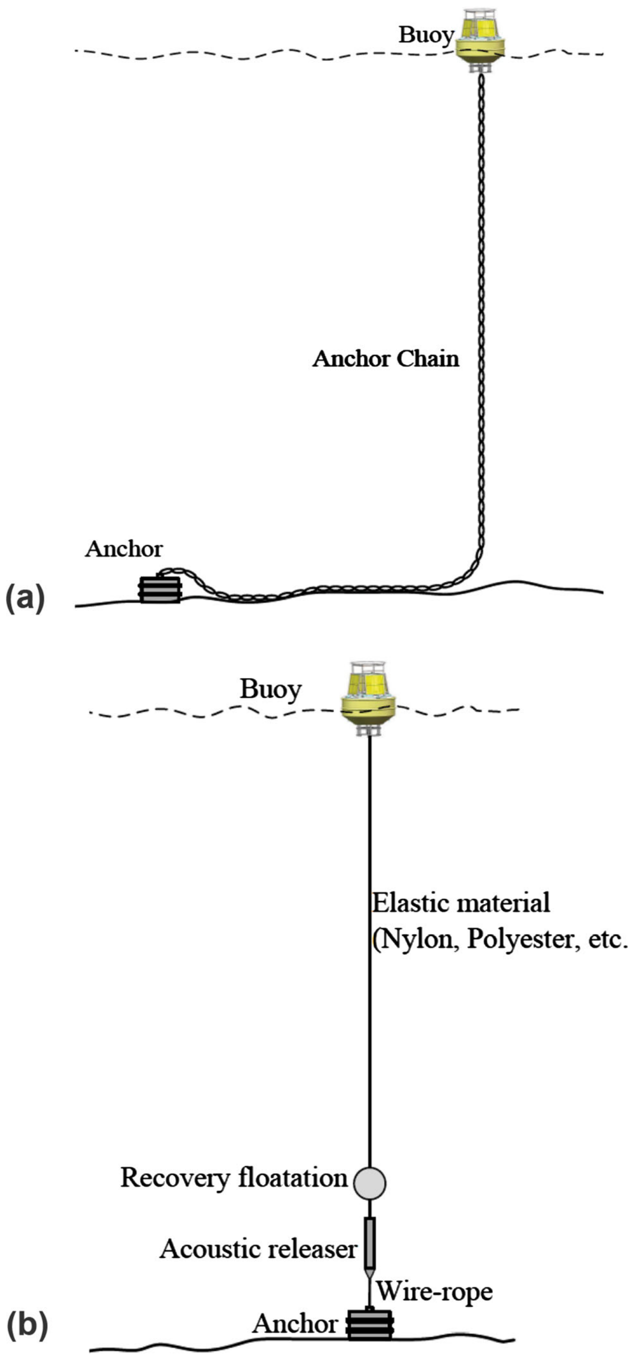

Fig. 1 (**a**) Catenary mooring, and (**b**) Semi-taut mooring [2]

components of a mooring system which mainly consists of wire ropes and chains. Mostly, fatigue failure behavior is observed in mooring chains which is a result of loads encountered on the chains from cyclic loads resulting rom waves and tide, in addition to the high tension loads present from the stationed structure [1].

Currently, floating structures are required to be established in regions located further offshore, and into deep water, thus mooring systems with complex designs are

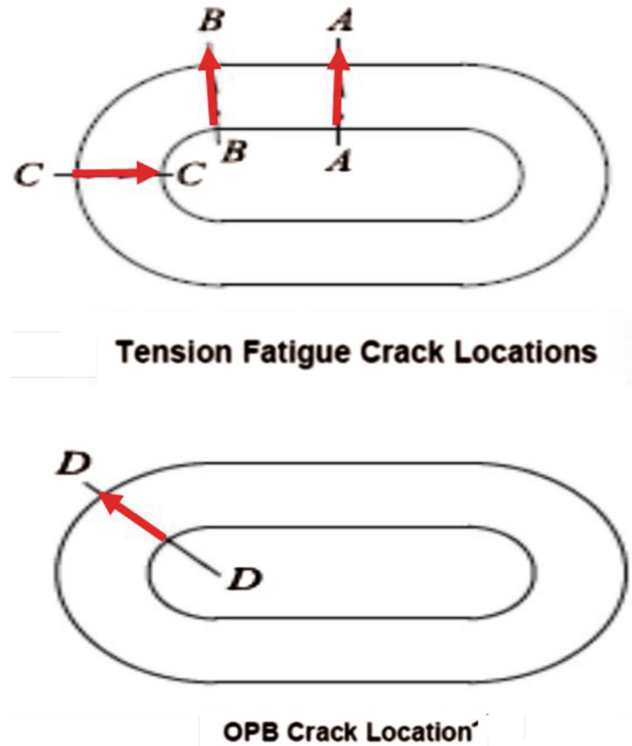

Fig. 2 Crack locations for Tension vs OPB Loading [10]

increasingly required to overcome the harsh working environment. This increased degree of complexity leads to a greater number of potential failure modes. Failure modes can be classified into two categories: mechanical and corrosive. The influence of seawater on mooring system chains was studied and the study concluded that there is an evident decrease in the fatigue life due to the dual effect of fatigue and corrosion in the so called corrosion-fatigue damage mechanism [3].

Mooring system components, chains, anchors and connecting elements, must be chosen with consideration of the mooring configuration, location and the requirements of a long term mooring [4]. Requirements for these components are discussed in the offshore standard DNV_OS_E302 [5]. According to standard specification, mooring chains are usually made of cold rolled steel bars from grades R3, R3S, R4, R4S, and R5.

The stress and failure analysis of the mooring systems has received the attention of several investigations. Rampi et al. [6] concluded that the fracture of the chain link can be located in four various regions depending on the loads and stresses applied. For instance, if the chain is being subjected to tension fatigue, cracks may be identified at the crown, bend, and straight portion of the chain. If the chain is also examined for out of plane bending (OPB), the cracks are most observed between the bent portion and the crown, as OPB is caused by both stress and rotation, see Fig. 2.

OPB fatigue mechanism was found to act as the root cause of the short service life deep water buoy mooring chains. This mechanism, illustrated in Fig. 3, uses the stress histogram applied to the mooring chain including chain rotation effect. Several failures occur in the chain conveyors due to different causes [7, 8].

The current study is on a 150-m chain which is composed of five studded links, 30 m each, connected to each other using a shackle. This mooring system was installed at the red sea near a region called Abou Zenima. This chain is attached to a 4 tons anchor on the seabed, and to a single buoy mooring link on the other end. After only three days of installation, the chain fractured at the single buoy mooring link end, near the midway of the first free chain link, see Fig. 4a. The environmental conditions associated with the failure are wind speed of ± 23 m/s, and NNW at swell ± 2.5 m. The chain fractured at the locations where the crown and shank intersected, as shown in Fig. 4. The broken chain was investigated by visual examination, metallographic examination, and scanning electron microscopy.

The chemical composition and mechanical properties of the failed part were also identified and compared with the design specifications. The results of this investigation are presented hereafter. Based on location of failure, the failure occurs at location where out of plan bending and tension overload are the main purposes of failure where tension overload is localized between both the crown and the shank while out of Plane Bending is localized near the shank zone, as illustrated in Fig. 4.

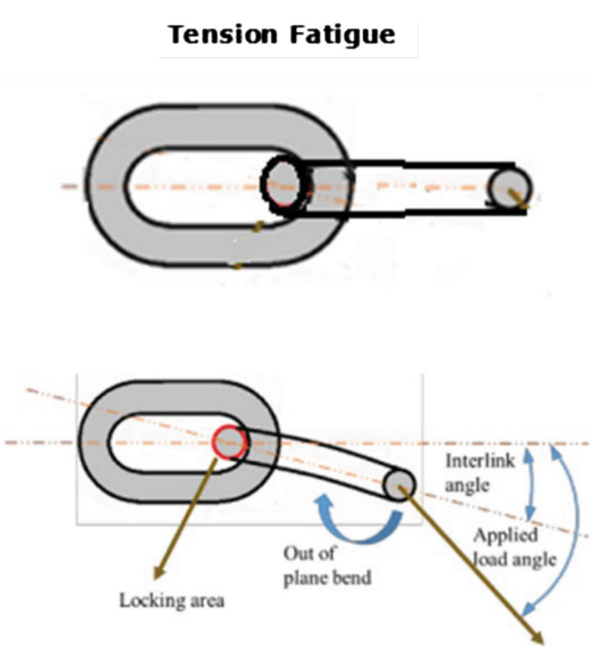

Fig. 3 Tension fatigue vs Out of Plane Bending (OPB) mechanism [10]

Experimental Work

The failed chain link was put under several tests to validate and characterize the material and understand the failure mode. The chemical composition of the chain link used in this study is shown in Table 1. Metallography samples were sectioned from regions away from the failure specimens. These sectioned samples were ground, then polished to a fine finish. Finally, the samples were etched using NITAL 2% to reveal the grains and other microstructure features.

As for tensile testing, a specimen was machined to be as close as possible to the required dominions mentioned by the ASTM-E8 standard, see Fig. 5. The tensile test was conducted using SHIMADZU/UH-1000KN Universal Testing Machine. Analysis of fracture surface was executed using QUANTA FEG 250 scanning electron microscope, coupled with energy-dispersive x-ray (EDX). Finally, the hardness values were evaluated using Zwick/Roell ZHU250.

Results and Discussion

Material and Fracture Characterization

Observation of the fracture surface of the failed chain was conducted to understand the possible failure mechanism. As illustrated in Fig. 4a, the surface examination of the fractured surface of the chain revealed a brittle and a corroded surface (left side) where crack propagates from top to bottom as illustrated in Fig. 4a by red-dashed arrow. On the other hand, fracture at shank zone also showed a brittle manner with corrosion pits near the center of the chain, see yellow-dashed circles in Fig. 4a (right side).

According to the International Association of Classification Society (ICAS), chains that form links used in mooring systems are manufactured from high strength steel which are classified according to the minimum ultimate tensile strength into five grades: R3, R3S, R4, R4S and R5 [10]. Table 2 illustrates the minimum tensile strength properties for the most used steels used for mooring chains and the tensile and hardness results for the original sample prepared from the failed chain link. The results illustrated in Tables 1 and 2 are comparable to the results of R3 steel. The tensile strength results for original samples are lower than R3 steel which is linked to lower carbon content of chain sample compared to R3 steel.

Optical micrographs of the investigated samples show the presence of ferrite and pearlite, see Fig. 6. Corrosion pits filled with iron oxides were also observed on the chain fracture surface, illustrated in Figs. 4a and 6. These pits were formed due to corrosion which is accelerated due to

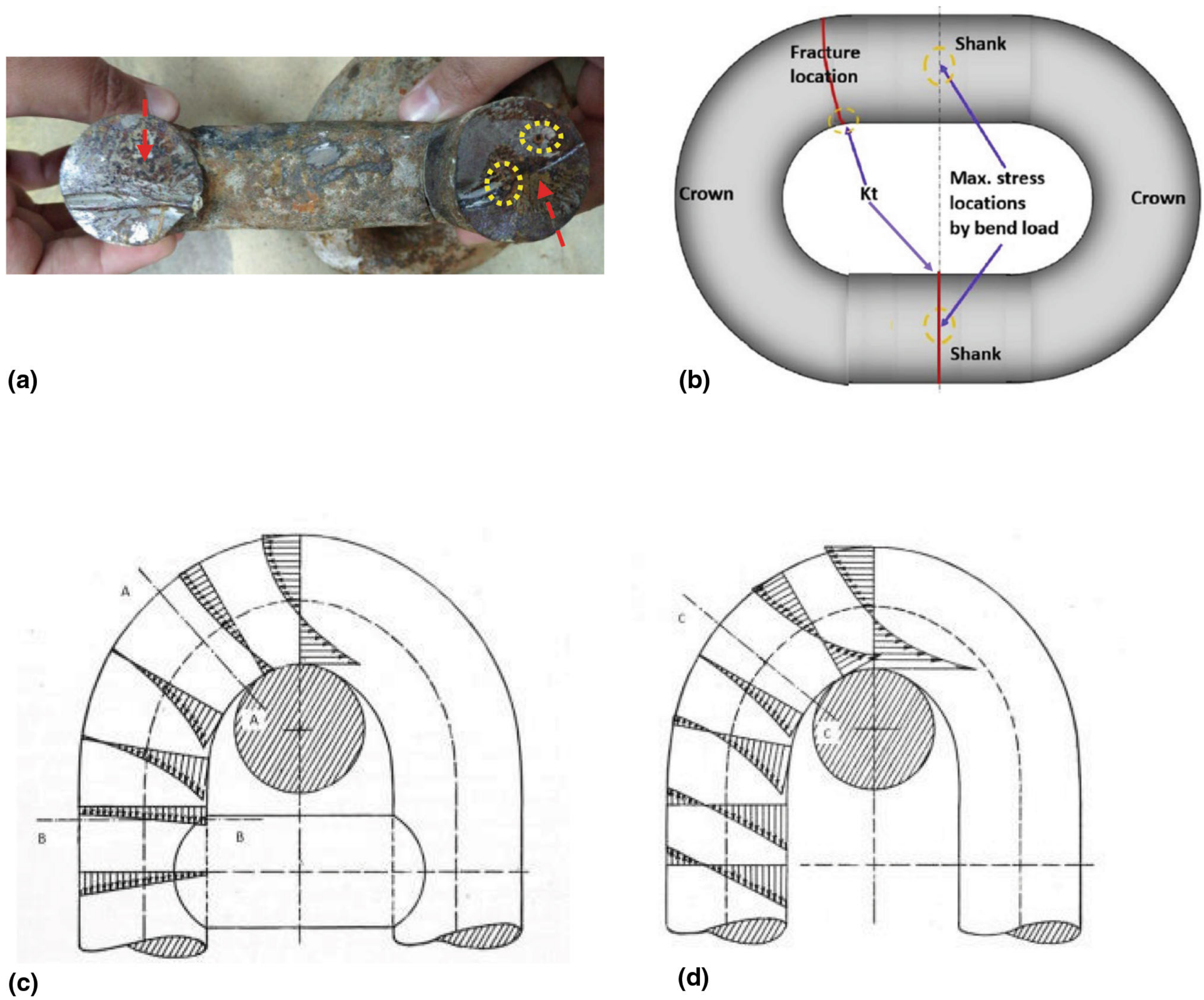

Fig. 4 (**a**) Fractured chain link, (**b**) Schematic of link chain stresses and fracture locations, (**c**) bending, and (**d**) tensile distribution of stresses in a chain [9]

Table 1 Composition of the steel chain link used in this study

Element		C	Si	Mn	P	S	Mo	Ni	Cr	Fe
wt.%		0.21	0.56	1.51	0.011	0.02	0.009	0.069	0.008	97.254
Standard (R3)	% Min.	0.23	0.2	1.6	0	0	0	0	0	Bal.
	% Max.	0.27	0.35	1.9	0.02	0.02	0.008	0.4	0.35	

presence in sea water environment. Local pitting corrosion is mostly observed in the submerged near-surface zone which initiate around inclusions of MnS and TiVCr [11]. These pits cause significant mass loss resulting in local stress concentration and initiate cracks under force which lead to accelerated degradation of the mooring chains.

Figure 5c illustrates that the fracture surfaces of the tensile sample is ideal cup and cone fracture which indicates ductile behavior when overloading. This was verified with SEM images for the tensile fracture surface which shows equiaxed dimples indicating a ductile fracture manner, see Fig. 7.

Numerical Simulation Conditions

A model of the chain's configuration was generated by Solid works with the real dimensions of the studied chain. The model was then inserted into ABAQUS Simula 2018

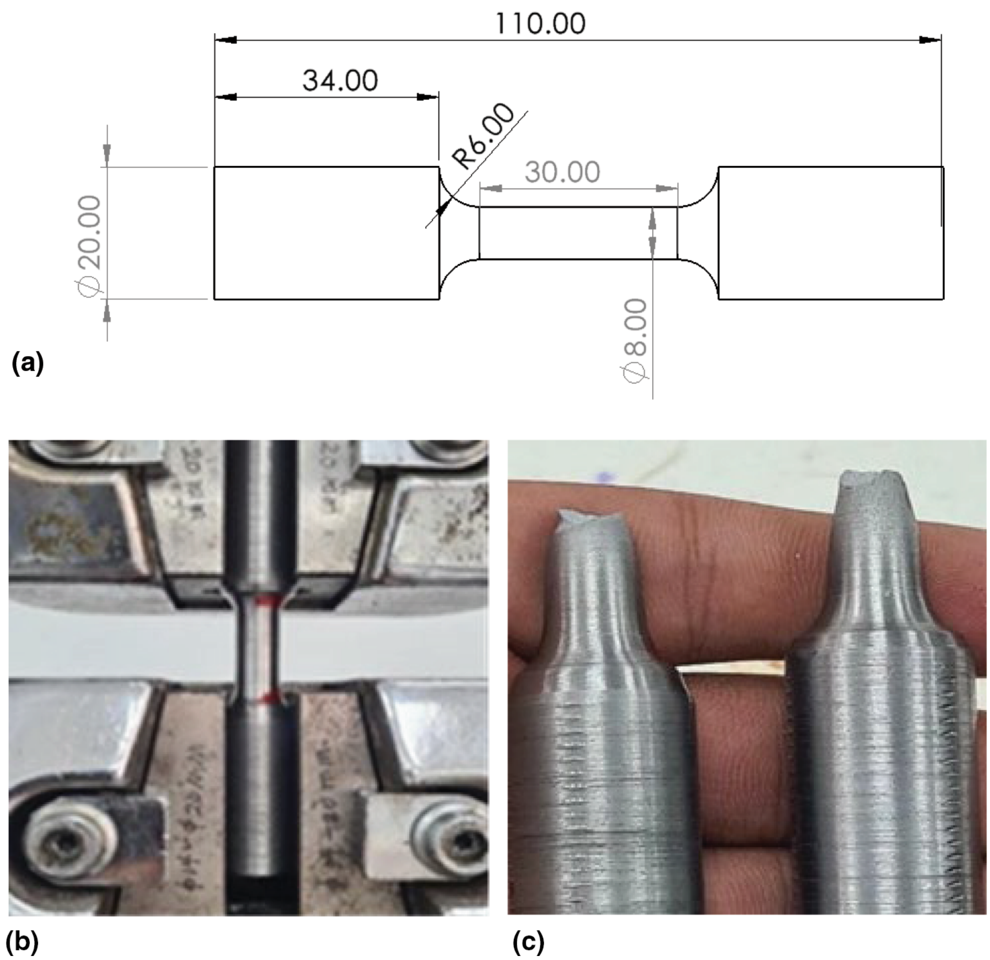

Fig. 5 (**a**) Schematic drawing for tensile test sample, (**b**) and (**c**) tensile test sample before and after test

Table 2 Mechanical properties for R3, R3S, R4 and chain sample

Steel grade	UTS (MPa)	YS (MPa)	Elongation %
R3 [5]	690	410	17
R3S [5]	770	490	15
R4 [5]	860	580	12
Failed sample	UTS (MPa)	YS (MPa)	Elongation %
	601	384	30
	Vickers hardness test (MPa)		
	Average HVN (MPa)		201

for finite element simulation. The finite element model, represented in Fig. 8, was created using a 3-chain links taking into consideration that every link is considered and treated as an individual link. The first step in the model was to insert accurately the material properties. The model has defined elastic and plastic data for deformation of the material, as shown in Fig. 9. The elastic and plastic data inserted for R3 steel is extracted from the data obtained from the tensile test.

3D computational domain was defined in the model to define the solver as explicit dynamic solver to accurately solve the computational analysis of the model. Thus, each link of the chain is discretized with 8 node linear brick solid, reduced integration elements (C3D8R). Figure 8 shows the mesh of the full assembly of the chain presented with the boundary condition. Two reference point are created with the chain's links using a coupling constrain. The chain is fixed from one of its free ends while the other end is given a displacement along the link direction. The displacement boundary condition is created on these two reference points. Figure 8 also illustrates the mesh of the assembly. Which was created on the links individually, every part includes 165,824 element and 31,364 nodes. Which in total of the assembly around 600,000.

Simulation results

Using the ABAQUS Simula 2018, the stress distribution was calculated under a displacement-force condition to ensure the stabilization of the simulation along with the

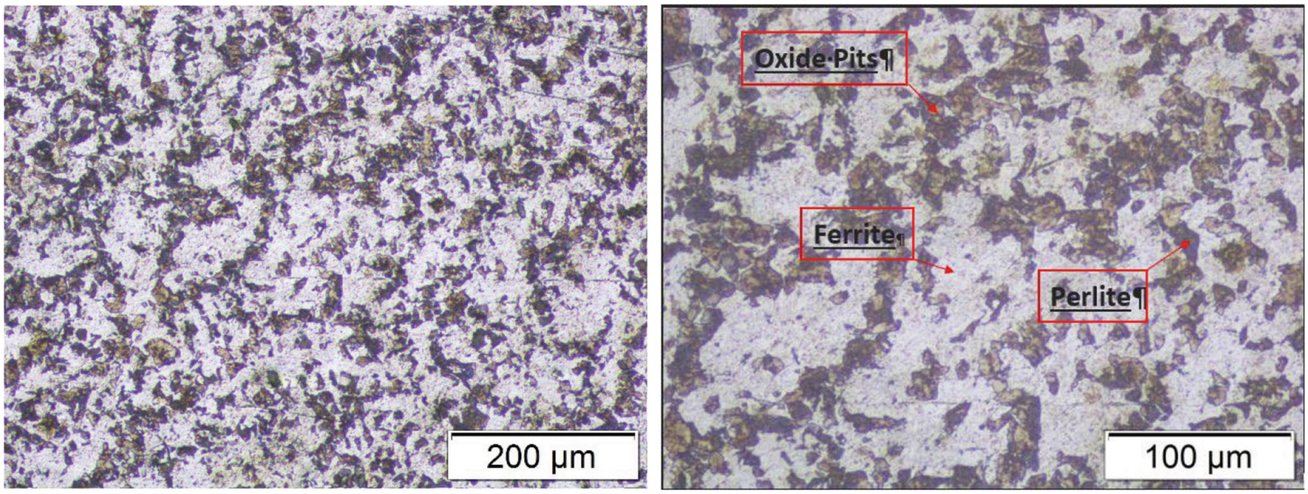

Fig. 6 Optical micrographs of chain link sample

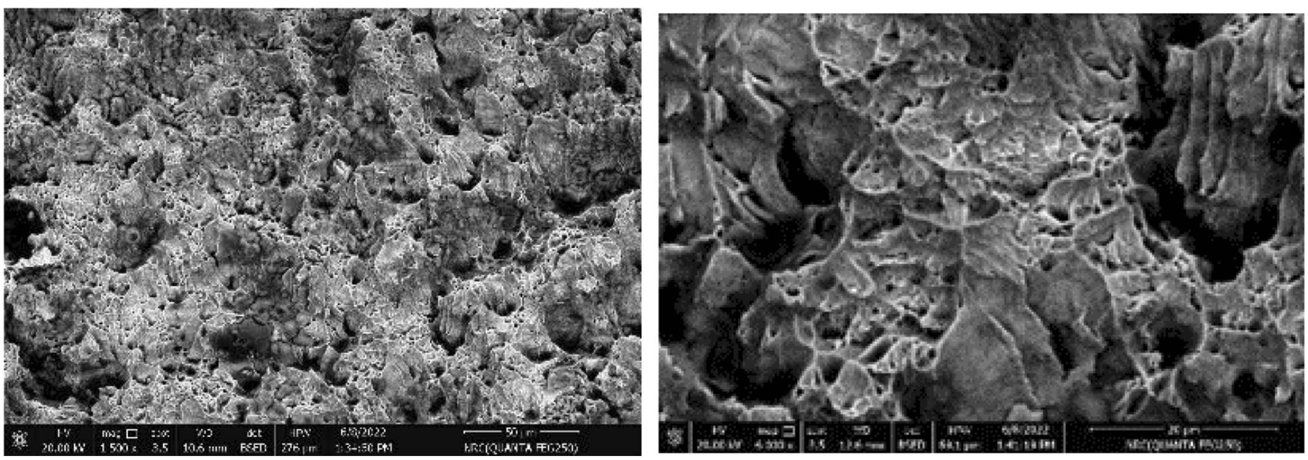

Fig. 7 SEM images of fracture surface of tensile test sample at different magnification

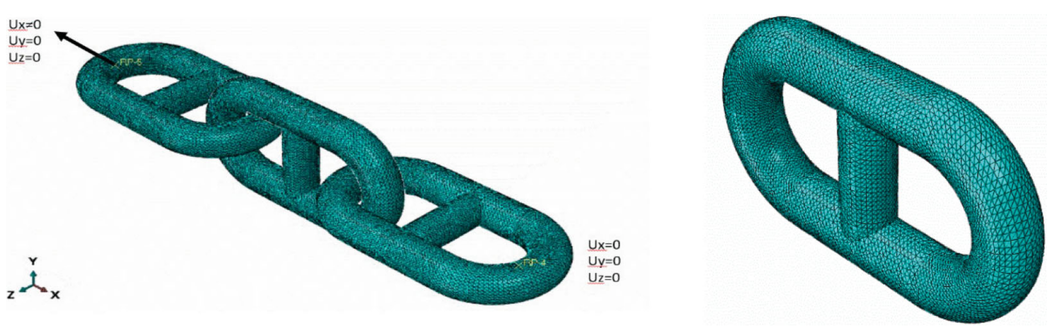

Fig. 8 3D models of mooring chain

accuracy of the results to be near the true conditions of the chain. Figure 10a shows the results of the ABAQUS analysis when conditions are met. From the numerical analysis, the results show that the maximum Von-Mises stress is around 790 MPa which exceeds the breaking load of R3 steel. Therefore, red marked zones are considered possible location for fracture to occur. These locations are the same exact location where the actual failure occurred. On the other hand, using R4 steel, which has a higher UTS of 860 MPa, shows a safer design for material selection, as the stresses generated at the same conditions compared to R3 steel are lower than breaking load of R4 steel.

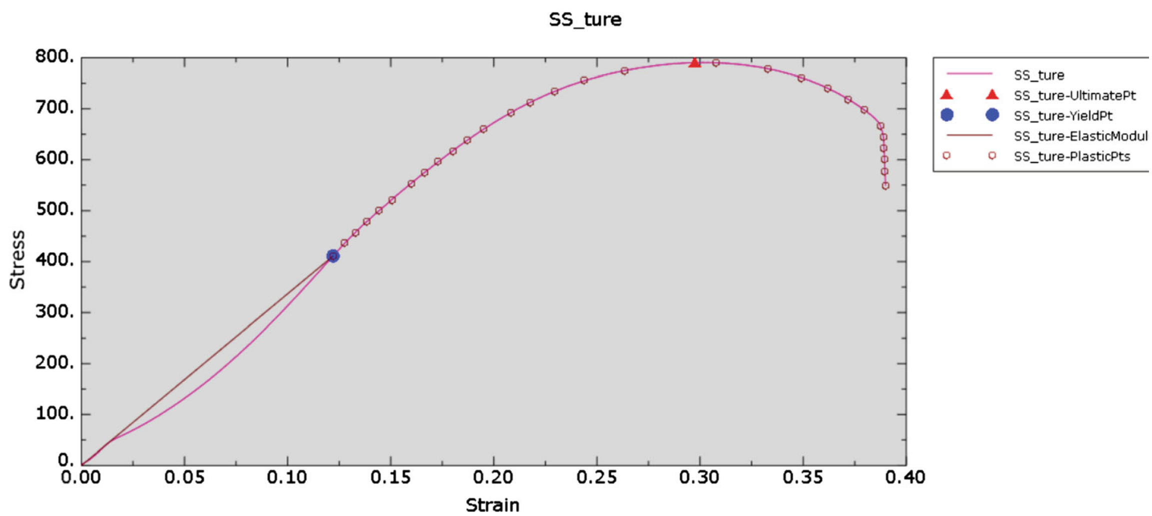

Fig. 9 Tensile properties of R3 steel generated from ABAQUS

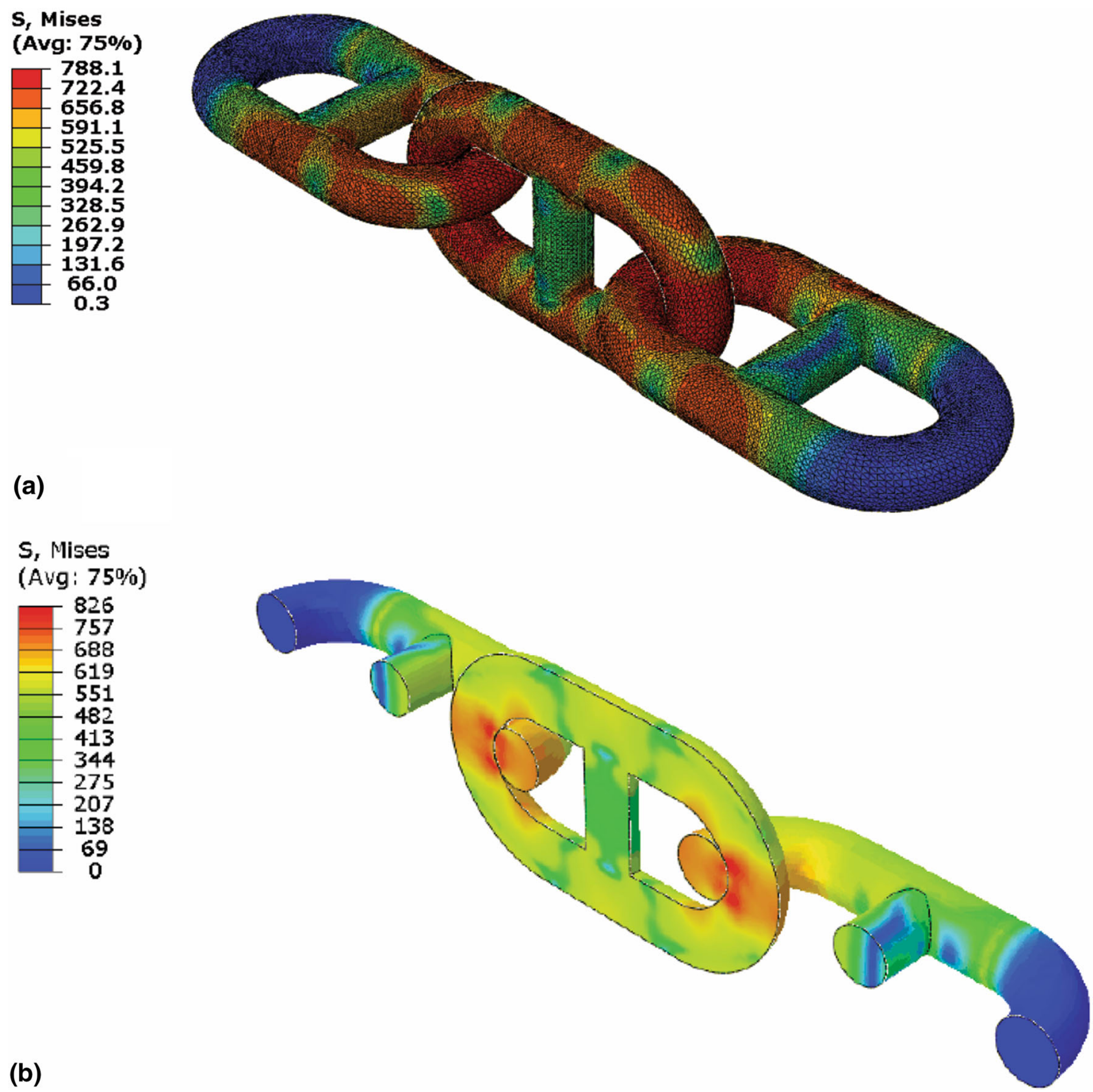

Fig. 10 Von-Mises stress distribution (**a**) R3 steel and (**b**) R4 steel

Conclusion

In this research, structural integrity of a mooring chain was investigated through ABAQUS Simula 2018. This was carried out for the prediction of the chain's material behavior and the calculation of maximum allowable load with respect to OPB loads. The results are summarized as follows.

- The microstructure confirmed that the material is low carbon alloy steel with ferrite and perlite grains along with iron oxide pits, which would be presumed to have made the material rather brittle.
- It was concluded that the failure might be due faulty material as chemical composition not conforming to the specified steel grade.
- Although, the fracture on the tensile sample shows ductile features, the fractographic analysis of the failed part reveals that the chain was fractured catastrophically in a brittle manner.
- FEA results are in accordance with the fractographic analysis.
- The results of finite element analysis of R3 steel show that the stress magnitude caused by OPB forces is 15% greater than that of ultimate tensile strength.
- R4 steel shows safer design compared to R3 steel.

Acknowledgments The authors acknowledge the Mechanical Testing Laboratory (MTL) Cairo University for conducting the mechanical tests.

References

1. K.-T. Ma et al., Chapter 2—types of mooring systems, in *Mooring system engineering for offshore structures*. ed. by K.-T. Ma (Gulf Professional Publishing, 2019), p. 19–39
2. J. Yu et al., Design and application of buoy single point mooring system with electro-optical-mechanical (EOM) cable. J. Mar. Sci. Eng. **8**(9), 672 (2020)
3. J. Fernández, W. Storesund, J. Navas, Fatigue performance of grade R4 and R5 mooring chains in seawater, in *International conference on offshore mechanics and arctic engineering*. (American Society of Mechanical Engineers, 2014)
4. R.E. Harris, L. Johanning, and J.J.M. Wolfram, Mooring systems for wave energy converters: a review of design issues and choices (2004)
5. D.N.V. AS, Offshore mooring chain. 2013, Standard DNV-OS-E302
6. L. Rampi et al,. Chain out of plane bending (OPB) fatigue joint industry project (JIP) static test program and OPB interlink stiffness. In ASME 2016 35th International Conference on Ocean, Offshore and Arctic Engineering (2016)
7. M. Hove, Growth of fatigue cracks in mooring line chains. NTNU (2016)
8. P. Jean, K. Goessens, and D. L'Hostis. Failure of chains by bending on deepwater mooring systems. In Offshore Technology Conference. OnePetro (2005)
9. E. Bjørnsen, Chains in mooring systems. Institutt for konstruksjonsteknikk (2014)
10. A. López et al., Tribocorrosion behaviour of mooring high strength low alloy steels in synthetic seawater. Wear. **338–339**, 1–10 (2015)
11. X. Zhang et al., Localized corrosion of mooring chain steel in seawater. Corros. Mater. Degrad. **3**(1), 53–74 (2022)